Azide–water intermolecular coupling measured by two-color two-dimensional infrared spectroscopy

Borek, Joanna ; Perakis, Fivos ; Kläsi, Felix ; Garrett-Roe, Sean ; Hamm, Peter

Abstract: We utilize two-color two-dimensional infrared spectroscopy to measure the intermolecular coupling between azide ions and their surrounding water molecules in order to gain information about the nature of hydrogen bonding of water to ions. Our findings indicate that the main spectral contribution to the intermolecular cross-peak comes from population transfer between the asymmetric stretch vibration of azide and the OD-stretch vibration of D2O. The azide-bound D2O bleach/stimulated emission signal, which is spectrally much narrower than its linear absorption spectrum, shows that the experiment is selective to solvation shell water molecules for population times up to 500 fs. The waters around the ion are present in an electrostatically better defined environment. Afterwards, 1 ps, the sample thermalizes and selectivity is lost. On the other hand, the excited state absorption signal of the azide-bound D2O is much broader. The asymmetry in spectral width between bleach/stimulated emission versus excited absorption has been observed in very much the same way for isotope-diluted ice Ih, where it has been attributed to the anharmonicity of the OD potential.

DOI: https://doi.org/10.1063/1.4726407

Azide–water intermolecular coupling measured by two–color two-dimensional infrared spectroscopy

Joanna Borek[1], Fivos Perakis[1], Felix Kläsi[1], Sean Garrett-Roe[2], Peter Hamm[1]

[1] *Physikalisch-Chemisches Institut, Universität Zürich,*

Winterthurerstrasse 190, CH-8057 Zürich, Switzerland and

[2] *Department of Chemistry, University of Pittsburgh,*

*Chevron Science Center, 219 Parkman Avenue, Pittsburgh, PA 15260**

(Dated: September 18, 2012)

Abstract

We utilize two–color two-dimensional infrared spectroscopy to measure the intermolecular coupling between azide ions and their surrounding water molecules in order to gain information about the nature of hydrogen bonding of water to ions. Our findings indicate that the main spectral contribution to the intermolecular cross–peak comes from population transfer between the asymmetric stretch vibration of azide and the OD–stretch vibration of D_2O. The D_2O bleach/stimulated emission signal, which is spectrally much narrower than its linear absorption spectrum, shows that the experiment is selective to solvation shell water molecules for population times up to ∼500 fs. The waters around the ion are sitting an electrostatically better defined environment. After ∼1 ps, the sample thermalizes and selectivity is lost. On the other hand, the excited state absorption signal of D_2O is much broader. The asymmetry in spectral width between bleach/stimulated emission versus excited absorption has been observed in very much the same way for isotope–diluted ice Ih, where it has been attributed to the anharmonicity of the OD potential.

*Electronic address: phamm@pci.uzh.ch

I. INTRODUCTION

Due to its biological importance and presence of physical anomalies, water is the most studied liquid to date. However, questions remain about the dynamical process of solvation and involvement of water as a solvent in chemical processes [1]. What is of particular interest is dynamical and structural information on how water in a solvation shell rearranges, exchanges with bulk liquid and forms and breaks hydrogen bonds with the solute and bulk. This would shed light on how water is directly involved in progression of a chemical reaction or a biological process [2–4].

Currently, the dominant picture of water reorientation in both bulk and around hydrophobic solutes is the jump mechanism put forward by Laage and Hynes [5, 6]. In this perspective, water reorients via large angular jumps, exchanging hydrogen bond partners in a concerted manner. The mechanism is predicted to be the same in bulk water and around hydrophobic molecules. In solutions, the slightly slower reorientation of solvation shell waters in comparison to bulk water is attributed to an excluded volume effect. Recently, the jump mechanism has also been experimentally validated for ionic solutions via polarisation–selective two-dimensional infrared (2D–IR) spectroscopy [7].

This contrasts with the "dynamical iceberg" theory, as presented by Rezus and Bakker [8]. There, with the aid of infrared pump–probe spectroscopy, the authors observe a significant (almost an order of magnitude) slow down of solvation shell water reorientation times in highly concentrated solutions, as compared to bulk water. The "dynamical iceberg" term was coined since the solvation shell structure is bulk water–like, however, the extent of dynamical retardation resembles that of ice.

In the above mentioned experiments, time–resolved vibrational spectroscopy has proven to be an essential tool in observing ultrafast motions of molecules, including bulk water dynamics or solute–solvent interactions [7–20]. This is since the hydroxyl stretch has been directly associated with hydrogen bonding strength and thus providing a means to observe the bond strength between the ion and water [21–23]. Therefore, it is a suitable 'sensor' for any rearrangement within the ion's solvation shell.

Here, we measure the coupling of a molecular ion to water molecules directly hydrogen bonded to the ion to probe the solvent's response upon excitation. To that end, we utilize 2–color 2D–IR spectroscopy in which excitation of asymmetric stretch of azide (N_3^-) is followed

by probing in the OD–stretch frequency range. This very idea has been put forward in a recent paper by Zheng and coworkers [16], where neat D_2O and HOD/H_2O solutions of KSeCN have been investigated using high–power 2–color 2D–IR spectroscopy. However, in Appendix A, we show that their experiments measure the intramolecular coupling with a combination band of $SeCN^-$, which has an accidental degeneracy with the OD–stretch vibration.

We nevertheless find the idea of Ref. [16] extremely intriguing, as it opens the possibility of designing extremely selective spectroscopy in higher order pulse sequences such as 3D–IR spectroscopy [24–26] by passing on coherences and/or populations from one molecule to another, similar to heteronuclear NMR. One experiment we have in mind is to transfer excitation from a molecular ion to solvation water by means of a first frequency dimension in a 3D–IR spectrum, and then measure effectively a 2D–IR spectrum of those water molecules in a selective manner that solvate the ion (this idea has been first formulated by Martin Zanni in Ref. [27]). We therefore set out to search for an alternative to $SeCN^-$ that does not suffer from the same problem. The closest analogue would be SCN^- with the combination bands well outside of the OD–stretch absorption region. However, we observed that the much lower oscillator strength in comparison to azide was not enough to measure intermolecular coupling with water using our setup. With N_3^-, we found such a molecular ion that not only does not have interfering combination bands in the spectral region of interest, but also its high extinction coefficient of the asymmetric stretch vibration was advantageous for the studies undertaken.

II. MATERIALS AND METHODS

A commercial Ti:sapphire oscillator and chirped pulse amplifier delivered ultrafast 800 nm pulses of energy 1 mJ at 1 kHz repetition rate. Two homebuilt optical parametric amplifiers (OPA's) [28] were used to generate 2-2.7 μJ tunable compressed mid-IR pulses of 300 cm^{-1} bandwidth and $\sim$65 fs duration each.

The 2D–IR spectra were collected using a Fourier transform setup in pump-probe geometry [29] with direct phase measurement and a fast scanning routine for data acquisition [30]. In brief, a pump pulse from one OPA entered an interferometer where the beam was split and a delay between the two arms (coherence time t_1) was introduced and scanned over. A

second delay, the population time t_2, was introduced between the pump and probe pulses. Both beams were then overlapped in the sample and the probe beam was detected on a 32 pixels array MCT detector after dispersing it in a spectrograph. A Fourier transformation over the coherence time t_1 results in the pump frequency axis, ω_{pump}, whereas the probe axis, ω_{probe}, was detected directly. The pump frequency was centered at 2044 cm^{-1} and the probe at 2400 cm^{-1}. We used a closed volume sample cell with 1 M NaN_3 in D_2O solution sandwiched between two CaF_2 windows. No spacer was used, and the sample film was squeezed so that the maximum absorbance in the N_3^- asymmetric stretch and the OD–stretch regions did not exceed 0.3 OD. By observing interference fringes we align the two windows to be roughly parallel and thus guarantee a uniform sample thickness over the diameter of the laser beam. $KSe^{13}CN$ was synthesized by heating up $K^{13}CN$ with elementary selenium. All other chemicals were purchased from Sigma-Aldrich and used without further purification.

III. RESULTS

A. Linear spectra

Upon addition of high solute concentrations, the hydrogen bond network of water is perturbed and the changes are reflected in the OD–stretch absorption region [7, 31, 32]. Fig. 1 shows the linear spectra of 1 M NaN_3^- in D_2O solution along with the spectrum of pure D_2O to serve as a comparison. Upon addition of N_3^-, the OD–stretch absorption narrows and there is a slight blueshift in the maximum absorption. Moreover, two shoulders, at ca. 2450 and 2650 cm^{-1} are less pronounced. This is due to the fact that in the presence of a hydrophilic solute, the water molecules are present in a more defined configuration in comparison to the bulk and thus sample over a smaller frequency range. The blue shift in maximum absorption has been assigned to a signature of broken hydrogen bonds [31, 32]. However, there is no splitting in the hydroxyl stretch region, as it is observed in perchlorate or pseudohalide ion solutions [7, 16], where it is thought that solvation and bulk waters have such distinct vibrational frequencies that the OD–stretch band is separated into two peaks. In the case of N_3^-, no such distinction between bulk and solvation waters can be made by linear absorption spectroscopy.

B. 2D–IR spectra

2D–IR spectra always come as pairs of peaks with opposite signs, as indicated by the color code in Fig. 2: blue – bleach and/or stimulated emission, red – excited state absorption. If the same oscillator is pumped and probed after a certain population time t_2, one speaks of diagonal peaks and if coupling between two vibrations at different frequencies is observed, one speaks of cross–peaks. The present experiment is a two–color 2D–IR experiment with pump and probe pulse not spectrally overlapping, so the signal shown in Fig. 2 represents an intermolecular cross–peak between the asymmetric stretch vibration of N_3^- and the OD–stretch vibration of D_2O. The signal evolves in time from $t_2 = 300$ fs to $t_2 = 1200$ fs both in terms of the signal intensity as well as in terms of the width of the peaks. Initially, a weak bleach/stimulated emission signal is present (blue peak in Fig. 2), coinciding with maximum linear absorption in the OD–stretch region, as marked by the blue dashed line in Figs. 1 and 2. This bleach is spectrally narrow (<130 cm^{-1} full-width at half maximum (FWHM)) in comparison to the linear absorption spectrum of the OD–stretch vibration (300 cm^{-1} FWHM). The bleach contribution broadens, gains intensity (compare spectra at $t_2 = 300$ and $t_2 = 400$ fs), and, after ca. 1 ps, becomes the main spectral contribution. The excited state absorption (red peak in Fig. 2) is exceptionally broad (>250 cm^{-1}) in comparison to the bleach at early times. Moreover, unlike the bleach contribution, the excited state absorption peak initially has a plateau but then steadily decays with time (Fig. 4).

To discriminate inter- from intramolecular couplings (as it is the case for $SeCN^-$ in D_2O, see Appendix A), we performed the experiment for N_3^- solutions in both D_2O and H_2O. Fig. 3 shows a 1D cut from the corresponding 2D–IR spectra, with no detectable signal in the H_2O case. Thus we can confirm that the measured cross–peak is in fact of intermolecular coupling between the N_3^- and D_2O.

We would like to add that with our current signal-to-noise level, we were not able to measure any cross peak in a HDO:H_2O mixture for a low enough deuteration level, for which one would get mostly HOD with only negligible admixture of D_2O (i.e., ≈10% D_2O in H_2O).

IV. DISCUSSION

To analyze the origin of the two cross–peak contributions, we will first concentrate on the 2D–IR spectrum at $t_2 = 400$ fs. In the following, two possible mechanisms giving rise to a cross–peak will be discussed – direct coupling and population transfer [33] – and we will argue that the second mechanism dominates in the present case. Direct coupling can be described by the following expression for the energies of vibrational eigenstates, which can be calculated from an anharmonic perturbative treatment of the potential energy surface [34]:

$$E = \sum_i \hbar\omega_i \left(n_i + \frac{1}{2}\right) + \sum_{ij} x_{ij} \left(n_i + \frac{1}{2}\right)\left(n_j + \frac{1}{2}\right) \tag{1}$$

Here, ω_i are the harmonic frequencies, x_{ij} the anharmonic constants and n_i the number of vibrational quanta deposited in mode i. In a local mode representation, a simple model leading to the above expression is the exciton Hamiltonian with a coupling term β and local–mode anharmonicity Δ_i:

$$H = \left(\begin{array}{c|cc|ccc} 0 & & & & & \\ \hline & \hbar\omega_1 & \beta & & & \\ & \beta & \hbar\omega_2 & & & \\ \hline & & & 2\hbar\omega_1 - \Delta_1 & 0 & \sqrt{2}\beta \\ & & & 0 & 2\hbar\omega_2 - \Delta_2 & \sqrt{2}\beta \\ & & & \sqrt{2}\beta & \sqrt{2}\beta & \hbar\omega_1 + \hbar\omega_2 \end{array}\right) \tag{2}$$

Diagonalization of that Hamiltonian gives the eigenstates in Eq. 1.

In a 2D–IR spectrum, the anharmonic constants x_{ij} are directly related to the separation between the doublet of bands with opposite signs [27]. That is illustrated in Fig. 5, which schematically shows the energy level scheme of two oscillators. States are labeled as $|n_1 n_2\rangle$, where n_1 is the number of vibrational quanta deposited on the asymmetric stretch vibration of N_3^- and n_2 is the number of quanta deposited on the OD–stretch vibration. By the choice of the pump pulse frequency, we excite the $|10\rangle$ state selectively. The probe pulse may then excite the system further into the $|11\rangle$ state by depositing an additional quantum into the OD–stretch vibration of D_2O. If both states were directly coupled, the frequency of the $|10\rangle \rightarrow |11\rangle$ transition would differ from that of a direct excitation of one quantum of the OD stretch vibration $|00\rangle \rightarrow |01\rangle$ by the corresponding anharmonic constant x_{12}. As

the separation of the two peaks is large (≈200 cm^{-1}, see Fig. 2), this anharmonic constant would also have to be large.

Depending on the size of the coupling constant β, weak ($\beta \ll |\hbar\omega_2 - \hbar\omega_1|$) and strong ($\beta \gtrsim |\hbar\omega_2 - \hbar\omega_1|$) coupling limits are usually discussed [27]. Playing with the parameters in Eq. 2, one can easily verify that in the weak coupling limit it is impossible to create such a large off–diagonal anharmonicity of ≈200 cm^{-1}. On the other hand, if the coupling between N_3^- and D_2O molecules would be strong, then there should be a significant shift of the N_3^- asymmetric stretch vibration when changing from D_2O to H_2O, which is however not observed.

We therefore conclude that direct coupling plays only a minor role, and that it is population (energy) transfer which gives rise to the experimentally observed cross–peak. Population transfer is indicated by the dotted black arrows in Fig. 5. In the present case, population transfer is an uphill process with a relatively unfavorable maximum probability p_{OD} for exciting the OD excited state, for which we can give an upper limit determined by the energy gap between two transitions:

$$p_{OD} \leq \exp\left[-\frac{\hbar\,(\omega_2 - \omega_1)}{k_B T}\right] \simeq 8\% \tag{3}$$

Alternatively, the sample will relax back into the ground state with rate T_1 with the excess energy being deposited as heat. Due to low population transfer yield, heating effects will play a significant role in the measured 2D–IR spectra, which will be discussed further down in this section.

Fig. 4 shows the time-dependence of the 1-2 excited state absorption, that serves as a measure of the population of the D_2O excited state. The intensity of that band rises very quickly and is essentially fully established already after 250 fs (i.e., the earliest population time for which artifacts from the pulse overlap are sufficiently small). At a first sight, this result is very counter-intuitive since typical population transfer times between vibrations are many picoseconds up to hundreds of picoseconds [13, 35–37]. However, the time it takes to establish a quasi-equilibrium of population and depopulation of the D_2O excited state is dictated by the fastest rate in the level scheme of Fig. 5, which is the T_1 relaxation rate of water. It was measured to be 200 fs for bulk H_2O fs [14], 350-400 fs for bulk D_2O [38, 39], and we assume that it is equally fast for water that is hydrogen-bonded to N_3^-. To quantify

the result to a certain extent, we fit the data in Fig. 4 with the following function:

$$p_{OD}(t) = -ae^{-t/\tau_1} + ae^{-t/\tau_2} \tag{4}$$

and obtain for the two time constants τ_1 =150 fs and τ_2 =1.7 ps. We take these fit values with a lot of caution, since they originate from de facto an extrapolation, in particular for τ_1 (by the choice of the fit function, we had forced the population to be zero at $t = 0$ and for $t \to \infty$). Modeling the rate equation scheme of Fig. 5, one indeed finds that the D_2O population should rise essentially with its T_1 relaxation time, and should decay with the T_1 relaxation time of N_3^-, provided that the population transfer rate k_T is the slowest of all processes. Indeed, the slower time constants τ_2 obtained from the fit agree reasonably well with the known T_1 relaxation time of N_3^- in D_2O (2.4 ps [40]), while the faster time-constant τ_1 comes out somewhat too fast. The difference might be attributed to the additional decay channel k_{-T}, which, since it is down hill, might be quite fast as well. However, given the uncertainty in the determination of the fast time constant in the fit, we cannot quantify the contribution of the transfer rate.

As population transfer from the N_3^- asymmetric stretch vibration, $|10\rangle$, to the OD–stretch vibration, $|01\rangle$, takes place, we expect to see a signal that is the same as if we had pumped that state directly. What counts now for the 2D–IR response is the diagonal anharmonicity x_{22} (an no longer the off-diagonal anharmonicity x_{12}), which is known to be large for hydrogen-bonded OD vibrators. In other words, if integrating out the ion's ω_{pump} frequency, the measured cross–peak can be thought of as a 1D pump–probe response of those water molecules that couple to the ion, i.e. of selectively the solvation water molecules. Worth noting at this point is the lack of a tilt of the cross–peak. Though both azide [12] and water [14] absorption bands are each inhomogeneously broadened, the cross-peak shows no correlation between them. Thus, integrating out the ω_{pump} axis does not lead to any loss of information.

Two features in that pump–probe signal are worth discussing. First, the bleach/stimulated emission signal is spectrally much narrower than the 1D absorption spectrum of D_2O. The broad bandwidth of the D_2O absorption spectrum reflects the very heterogenous hydrogen environments the various water molecules experience in bulk water, and in addition the splitting between symmetric and asymmetric stretch vibration. Part of the narrowing in the azide-D_2O cross peak could be due to breaking of the symmetry of the cou-

pled water molecule, i.e. a localization of the vibration, in which case the splitting between symmetric and asymmetric stretch vibration might diminish or disappear. However, the bandwidth of the cross–peak (130 cm^{-1}) is still less than that of the fully symmetry-broken vibration in HOD (170 cm^{-1}, data not shown), so localization cannot explain all of the narrowing. The narrow bandwidth of the cross–peak qualitatively matches predictions based on molecular dynamics simulations for the frequency distribution of OD's donating hydrogen bonds to large anions like I^- [41] and perchlorate [7], therefore suggests that coupling occurs only to the subset of water molecules in the first solvation shell. The red-shift of a hydrogen-bond is essentially a measure of the local electric field at the OH bond [41–43]. We therefore conclude from the narrower linewidth of the 2D IR bleach/stimulated emission signal that the water around the ion sit in an electrostatically better defined environment. On the other hand, the central frequency of the bleach/stimulated emission signal is about in the middle of the D_2O band, so in average, both types of hydrogen bonds are equally strong. In connection with molecular dynamics (MD) simulations along the lines of Refs. [44, 45], one will be able to study to what extent the narrower linewidth reflects the distribution of structures of N_3^--D_2O hydrogen bonds, that appears to be smaller than that of inter-water hydrogen bonds in bulk water. Note that this spectroscopy is selective to those water molecules that are directly hydrogen-bond to azide. One may therefore see a narrower linewidth despite the fact that overall speaking, addition of salt may increase the structural inhomogeneity, as manifested for example by a broader linewidth of HDO:D_2O for certain salt solutions [46].

The second striking feature is the unusual, much broader excited state absorption peak which has been observed before also in 2D–IR spectra of isotope diluted water. It is present in liquid water [47], but much more pronounced in isotope–diluted ice Ih due to the smaller amount of disorder [48–51]. This feature, appearing in both OD– and OH–stretch vibrations of HOD/H_2O and HOD/D_2O mixtures of ice, respectively [48], has been explained using a non–adiabatic treatment of the Lippincott-Schröder model [52] which is a one–dimensional model of a hydrogen bond and which seems to capture essential attributes of 1D and 2D IR spectra of hydrogen bonded species quite well. In ice Ih, the origin of the exceptional asymmetry in the width of the two 2D–IR peaks is the quantum–mechanical delocalization of the vibrational wavefunction in the $R_{O\cdots O}$ direction. This causes the large distribution of $O\cdots O$ distances and thus Franck–Condon like transitions in a wide range of frequencies. Consequently, the spectral width of the excited state absorption peak is a measure of the

anharmonicity of the hydrogen bond potential that appears to be similar for both types of hydrogen bonds, despite the fact that the vibration in D_2O bound to azide might still be delocalized to a certain extent.

Due to the energy gap between the N_3^- and the OD–stretch vibrations, population transfer is a low probability process and thus most of the excited $N_3{}^-$ ions will relax back to the ground state by T_1-relaxation, see Fig. 5. On the one hand, the low probability results in the relatively weak cross–peak signal strength we observe. On the other hand, energy redistribution into the bulk solution will eventually heat it up, resulting in a frequency blue shift of all water molecules due to an overall weakening of the inter-water hydrogen bonds [53–57] and consequently an increase of intensity of the blue band associated with ground state processes in the 2D–IR spectra. With the relaxation time of $N_3{}^-$ being T_1=2.4 ps [40], one would not expect the heating effects to emerge as early as less than 1 ps in diagonal 2D–IR spectra. Nonetheless, because of the low probability of population transfer, the weak cross–peak will be very quickly affected by even minor heating contributions and appear relative early in the spectra. At later population times, the bleach signal does not only gain intensity, but also broadens to reflect the linear OD–stretch absorption spectrum which is a manifestation of thermalization of the whole solution and thus a loss of solvation shell selectivity. In addition also energy transfer by exciton coupling, which is very efficient in neat water [14, 58], will lead to a loss of selectivity.

V. SUMMARY AND CONCLUSIONS

In this work, we have presented 2–color 2D–IR spectra of 1 M N_3^- solutions in neat D_2O. We find a cross–peak between the asymmetric stretch vibration of N_3^- and the OD stretch vibration. The mechanism giving rise to this cross–peak is not direct coupling, but rather population transfer from N_3^- to D_2O. Population transfer is energetically uphill in this case with a maximum yield determined by a Boltzmann factor of $\approx$8%.

Population transfer process allows us to treat the 2D–IR spectra as a 1D pump–probe signal of solvation shell waters. The spectrally narrow bleach is a result of selectivity of the coupling to the solvation shell only and thus the 2D–IR spectra exhibit the frequency distribution of solvation shell waters. The distribution of hydrogen bonds of solvation water molecules to the ion is narrower than that of inter-water hydrogen bonds in bulk water, but

in average the hydrogen bonds are equally strong. In connection with MD simulations, it will be interesting to see how these observations can be related to structural properties of these hydrogen bonds. Furthermore, a pronounced asymmetry in spectral width of excited state absorption and the bleach signal is found, very much like in isotope diluted ice Ih [48]. In ice Ih, this asymmetry has been attributed to anharmonic coupling of the OD vibration to the hydrogen bond vibration [48]. We therefore conclude that the hydrogen bond potentials between the N_3^- and a D_2O molecule have similar anharmonic properties as in ice Ih.

To sum up, 2–color 2D–IR spectroscopy reveals a very detailed picture of the structure of water-solute hydrogen bonds. It will be interesting to extend this work to 3D–IR spectroscopy. Just like the present experiment results in effectively a 1D pump-probe response of solvation water in a selective manner, a 3D–IR spectrum, in which the first frequency dimension labels the N_3^- stretch vibration and the second and third frequency dimensions the D_2O stretch vibration, would effectively be a selective 2D–IR spectrum, that would allow one to resolve the inhomogeneity of these hydrogen bonds and their dynamics.

Acknowledgments

The authors would like to thank Jan Helbing and Julien Réhault for inspiring discussions and their help with the experiments. We would also like to thank Rolf Pfister for synthesizing $KSe^{13}CN$. This work has been supported by the Swiss National Science Foundation through the National Center of Competence and Research (NCCR) MUST.

APPENDIX A: KSeCN and $KSe^{13}CN$ in D_2O

Ref. [16] claimed that intermolecular vibrational energy transfer between an ion and its aqueous solvation shell has been observed for $SeCN^-$ in D_2O, very much in the same way as for N_3^- in the present paper. Upon addition of large quantities (>10 M) of $SeCN^-$ ions to D_2O, the OD–stretch band is split into two. It is believed that the blue–shifted part of the spectrum corresponds to solvation shell waters with a broken hydrogen bond network and the red–shifted peak originates from bulk water [7, 16].

We show here that the results reported by Zheng *et al.* [16] have been misinterpreted and intramolecular coupling to an combination mode of $SeCN^-$ has been measured instead. First

evidence comes from $SeCN^-$ in H_2O (Fig. 6, green line), where one sees two sharp bands. From their frequencies [59], it is clear that the peak at ca. 2630 cm^{-1} is a combination mode of CN– and Se–C stretch vibrations ($\nu_3 + \nu_1$) and the band at ca. 2480 cm^{-1} is a combination band of CN–stretch and SeCN bend vibrations ($\nu_3 + \nu_2$). In comparison to the D_2O band, these combination mode are extremely weak in intensity (the green line in Fig. 6 has been up-scaled by a factor of ∼50, so the combination bands can no longer be identified in the presence of D_2O). Consequently, KSeCN and $KSe^{13}CN$ in D_2O reveal essentially the same spectra (Fig. 6, black and red spectra). Nevertheless, the more intense combination mode, $\nu_1 + \nu_3$, dominates the 2D–IR response (Fig. 7). Upon ^{13}C substitution, the cross–peak is shifted not only in the pump frequency, ω_{pump}, but also in the probe frequency, ω_{probe}. This is expected since the combination mode frequency shifts essentially the same way as the fundamental CN–stretch vibration. This is because ^{13}C labeling affects mostly the -CN fundamental vibration, so any combination mode that includes the -CN vibration shifts by essentially the same amount. Hence, what has been previously assigned to a cross–peak between the ion's CN-stretch band and the OD-stretch of D_2O [16] is in fact intramolecular direct coupling between the CN stretch and the combination band of SeC– and CN–stretches of KSeCN. In contrast, N_3^- used here does not have any combination band in the corresponding frequency range because it is symmetry forbidden, and no response is detectable when replacing D_2O by H_2O (Fig. 3).

---

[1] Science **309**, 78 (2005).

[2] B. Bagchi, Chem. Phys. Lett. **529**, 1 (2012).

[3] S. Combet and J. Zanotti, Phys. Chem. Chem. Phys. (2012).

[4] D. Zhong, S. K. Pal., and A. H. Zewail, Chem. Phys. Lett. **503**, 1 (2011).

[5] D. Laage and J. T. Hynes, Science **311**, 832 (2006).

[6] D. Laage and J. T. Hynes, J. Phys. Chem. B **112**, 14230 (2008).

[7] M. Ji, M. Odelius, and K. J. Gaffney, Science **328**, 1003 (2010).

[8] Y. L. A. Rezus and H. J. Bakker, Phys. Rev. Lett. **99**, 148301 (2007).

[9] H. Graener, T. Q. Ye, and A. Laubereau, J. Chem. Phys. **90**, 3413 (1989).

[10] H. Graener, G. Seifert, and A. Laubereau, Phys. Rev. Lett. **66**, 2092 (1991).

[11] H. Bian, H. Chen, J. Li, X. Wen, and J. Zheng, J. Phys. Chem. A **115**, 11657 (2011).

[12] P. Hamm, M. Lin, and R. Hochstrasser, Phys. Rev. Lett. **81**, 5326 (1988).

[13] H. Bian, X. Wen, J. Li, H. Chen, S. Han, X. Sun, J. Sing, W. Zhuang, and J. Zheng, Proc. Nat. Acad. Sci. **108**, 4737 (2011).

[14] M. L. Cowan, B. D. Bruner, N. Huse, J. R. Dwyer, B. Chugh, E. T. J. Nibbering, T. Elsaesser, and R. J. D. Miller, Nature **434**, 199 (2005).

[15] L. Piatkowski and H. J. Bakker, J. Chem. Phys. **135**, 214509 (2011).

[16] H. Bian, X. Wen, J. Li, and J. Zheng, J. Chem. Phys. **133**, 034505 (2010).

[17] A. Bakulin, M. Pshenichnikov, H. Bakker, and C. Petersen, J. Phys. Chem. A **115**, 1821 (2011).

[18] J. Zheng, K. Kwak, J. Asbury, X. Chen, I. R. Piletic, and M. D. Fayer, Science **309**, 1338 (2005).

[19] L. Liu, J. Hunger, and H. J. Bakker, J. Phys. Chem. A **115**, 14593 (2011).

[20] J. B. Asbury, T. Steinel, and M. D. Fayer, J. Phys. Chem. B **108**, 6544 (2004).

[21] G. C. Pimentel and A. L. McClellan, *The Hydrogen Bond* (WH Freeman and Co, 1960).

[22] M. Falk and T. Ford, Can. J. Chem. **44**, 1699 (1966).

[23] W. Mikenda, J. Mol. Struct. **147** (1986).

[24] F. Ding and M. T. Zanni, Chem. Phys. **341**, 95 (2007).

[25] S. Garrett-Roe and P. Hamm, J. Chem. Phys. **130**, 164510 (2009).

[26] S. Garrett-Roe, F. Perakis, F. Rao, and P. Hamm, J. Phys. Chem. B **115**, 6976 (2011).

[27] P. Hamm and M. Zanni, *Concepts and Methods of 2D–IR Spectroscopy* (Cambridge, 2011).

[28] P. Hamm, R. A. Kaindl, and J. Stenger, Opt. Lett. **25**, 1798 (2000).

[29] L. P. DeFlores, R. A. Nicodemus, and A. Tokmakoff, Opt. Lett. **32**, 2966 (2007).

[30] J. Helbing and P. Hamm, J. Opt. Soc. Am. B **28**, 171 (2011).

[31] G. Brink and M. Falk, Can. J. Chem. **45** (1970).

[32] J.-J. Max and C. Chapados, J. Chem. Phys. **115** (2011).

[33] M. Khalil and A. Tokmakoff, Chem. Phys. **266**, 213 (2000).

[34] G. Herzberg, *Molecular spectra and molecular structure, Vol II. Infrared and Raman spectra of polyatomic molecules* (Krieger, 1945).

[35] S. Woutersen, Y. Mu, G. Stock, and P. Hamm, Proc. Natl. Acad. Sci. USA **98**, 11254 (2001).

[36] M. Khalil, N. Demirdöven, and A. Tokmakoff, J. Chem. Phys. **121**, 362 (2004).

[37] H. Bian, J. Li, X. Wen, and J. Zheng, J. Chem. Phys. **132**, 184505 (2010).

[38] V. V. Volkov, D. J. Palmer, and R. Righini, J. Phys. Chem. B **111**, 1377 (2007).

[39] L. Piatkowski, K. B. Eisenthal, and H. J. Bakker, Phys. Chem. Chem. Phys. **11**, 9033 (2009).

[40] M. Li, J. C. Owrutsky, M. Sarisky, J. P. Culver, A. Yodh, and R. M. Hochstrasser, J. Chem. Phys. **98**, 5499 (1993).

[41] J. D. Smith, R. J. Saykally, and P. L. Geissler, J. Am. Chem. Soc. **129**, 13847 (2007).

[42] K. B. Moller, R. Rey, and J. T. Hynes, J. Phys. Chem. A **108**, 1275 (2004).

[43] D. Laage and J. T. Hynes, J. Phys. Chem. B **112**, 14230 (2008).

[44] S. Li, J. R. Schmidt, A. Piryatinski, C. P. Lawrence, and J. L. Skinner, J. Phys. Chem. B **110**, 18933 (2006).

[45] S. Li, J. R. Schmidt, and J. L. Skinner, J. Chem. Phys. **125**, 244507 (2006).

[46] M. F. Kropman and H. J. Bakker, Chem. Phys. Lett. **370**, 741 (2003).

[47] H. J. Bakker and H. K. Nienhuys, Science **297**, 587 (2002).

[48] F. Perakis, S. Widmer, and P. Hamm, J. Chem. Phys. **134**, 204505 (2011).

[49] G. Seifert, L. Weidlich, and H. Graener, Phys. Rev. B **56**, 14231 (1997).

[50] H. Iglev, M. Schmeisser, K. Simeonidis, A. Thaller, and A. Laubereau, Nature **439**, 183 (2006).

[51] A. M. Dokter and H. J. Bakker, J. Chem. Phys. **128**, 024502 (2008).

[52] E. R. Lippincott and R. Schroeder, J. Chem. Phys. **23**, 1099 (1955).

[53] K. J. Gaffney, I. R. Piletic, and M. D. Fayer, J. Phys. Chem. A **106**, 9428 (2002).

[54] K. J. Gaffney, P. H. Davis, I. R. Piletic, N. E. Levinger, and M. D. Fayer, J. Phys. Chem. A **106**, 12012 (2002).

[55] A. J. Lock and H. J. Bakker, J. Chem. Phys. **117**, 1708 (2002).

[56] A. Pakoulev, Z. Wang, and D. D. Dlott, Chem. Phys. Lett. **371**, 594 (2003).

[57] H. J. Bakker, A. J. Lock, and D. Madsen, Chem. Phys. Lett. **385**, 329 (2004).

[58] S. Woutersen and H. J. Bakker, Nature **402**, 507 (1999).

[59] V. Lenchenkov, C. She, and T. Lian, Phys. Chem. B **110**, 19990 (2006).

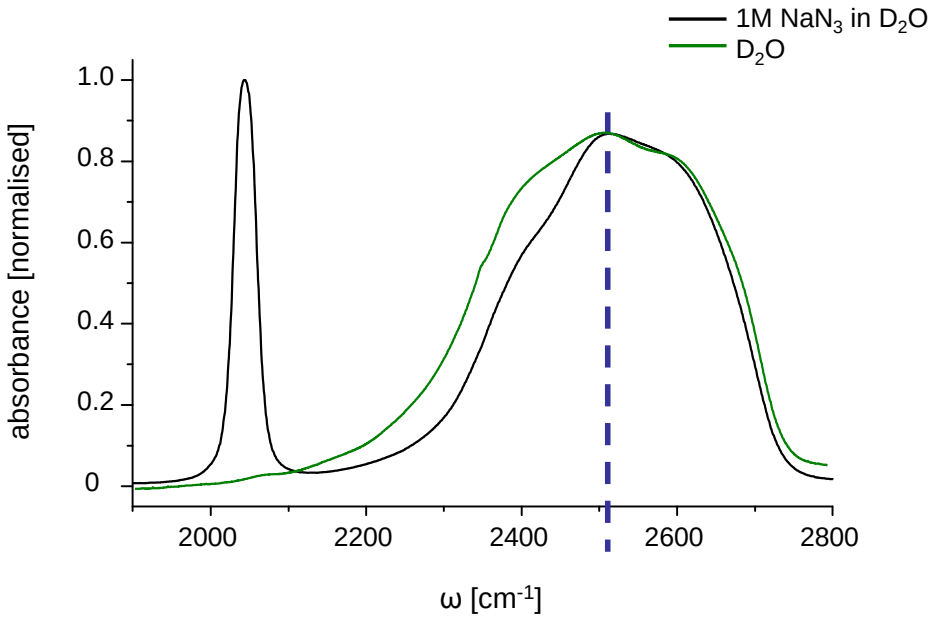

FIG. 1: Linear spectrum of 1 M N_3^- solution in D_2O (black line). The N_3^- asymmetric stretch vibration is found at 2044 cm^{-1} and the OD–stretch band is a wide, asymmetric peak with a maximum at $\sim$ 2510 cm^{-1} (blue dashed line). The OD–stretch band of pure D_2O (green line) is shown for comparison.

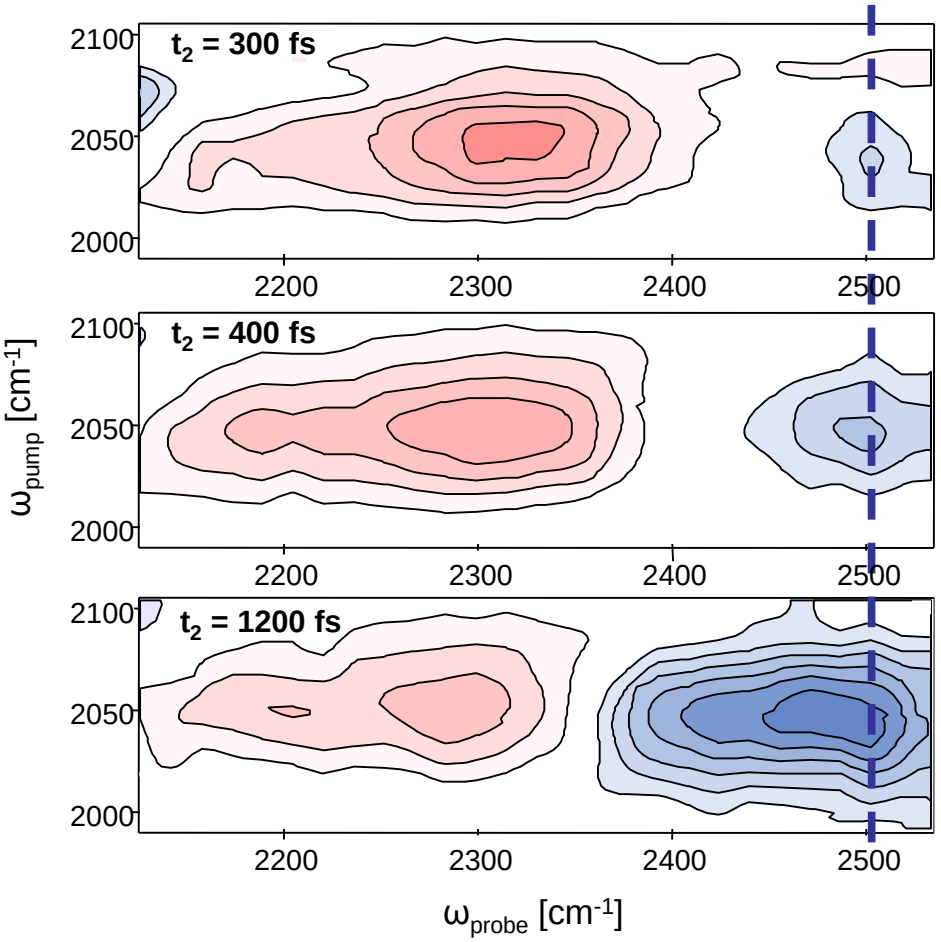

FIG. 2: 2–color 2D–IR spectra of N_3^- in D_2O at population times t_2 = 300, 400 and 1200 fs. Initially, a rather narrow and weak bleach/stimulated emission signal is observed (blue band), whose frequency coincides with the maximum of the linear absorption spectrum (blue dashed line, as in Fig. 1). Furthermore, a much broader excited state absorption signals is observed (red band). The bleach contribution grows in time, while the excited state absorption peak decays. After ∼1 ps, thermalization dominates in the form of a strong and wide bleach contribution.

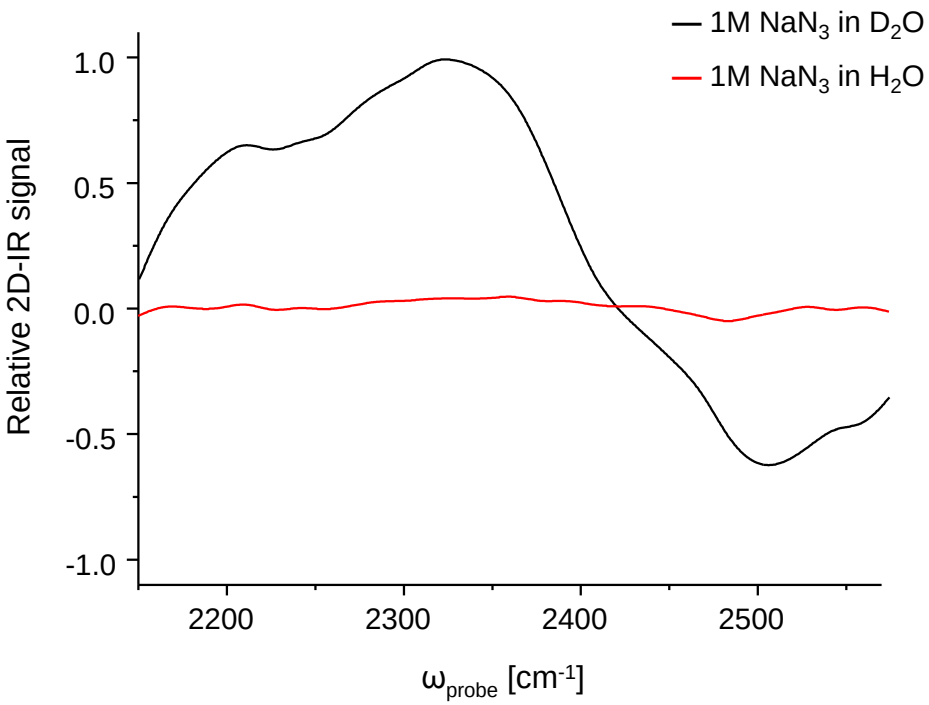

FIG. 3: Cuts of 2D–IR spectra at t_2=400 fs along ω_{pump}=2048 cm^{-1} comparing 2D–IR signal sizes for N_3^- in D_2O with N_3^- in H_2O. Since no 2D–IR response in H_2O is observed, the measured signal in D_2O originates from an intermolecular cross–peak.

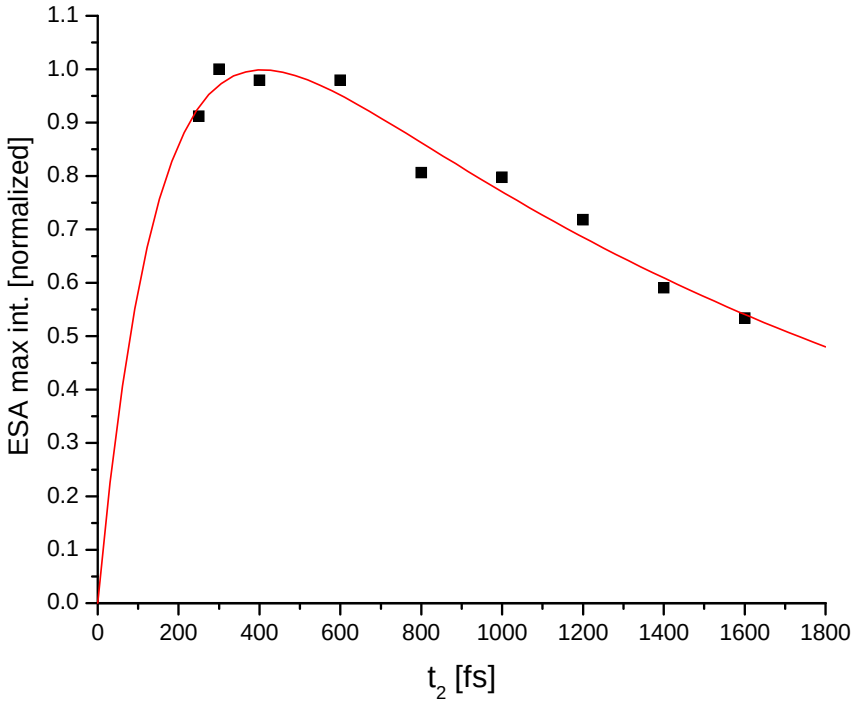

FIG. 4: Time dependence of the intensity of the peak of the 1-2 excited state absorption signal. The data are fit by Eq. 4, revealing the two time constants τ_1 =150 fs and τ_2=1.7 ps.

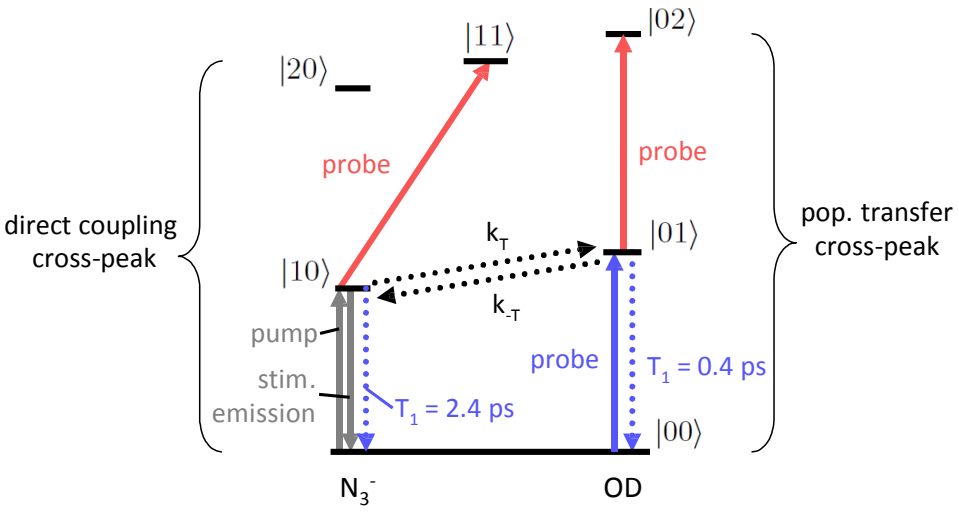

FIG. 5: Vibrational level scheme for coupled oscillators and the possible origins of 2D–IR cross–peaks. The symmetric stretch of N_3^- and OD-stretch are coupled and share a common ground state. The pump pulse induces a transition into the first excited state of the asymmetric stretch vibration of N_3^-. In the direct coupling case, the probe pulse moves the excitation up to the $|11\rangle$ state. In the case of population transfer, the oscillation moves from the $|10\rangle$ to the $|01\rangle$ state and the probe pulse induces further absorption into the $|02\rangle$ state.

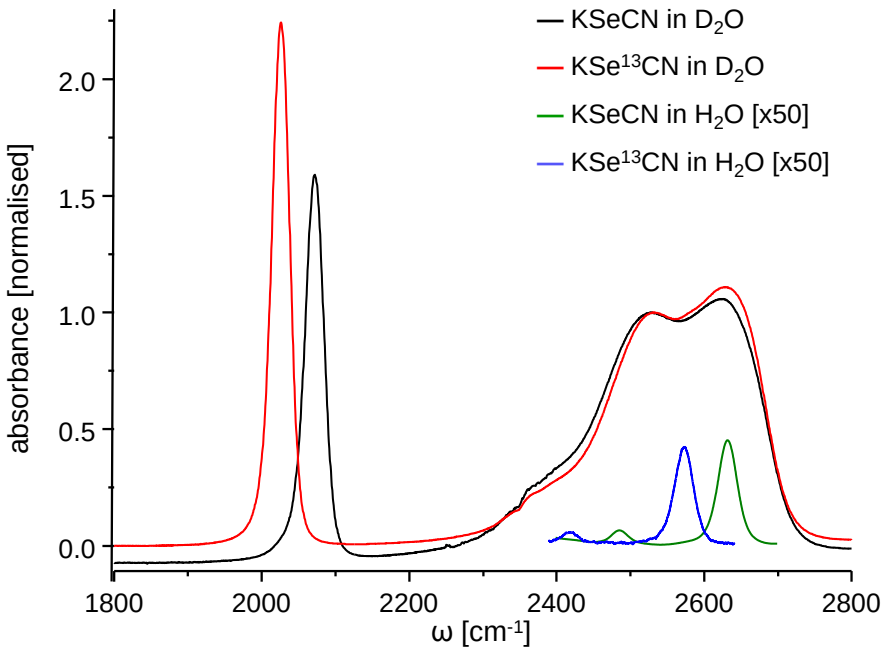

FIG. 6: Linear spectra of saturated KSeCN (black line) and KSe^{13}CN (red line) solutions in D_2O. CN-stretches are observed at 2070 and 2020 cm^{-1} for KSeCN and KSe^{13}CN respectively. The OD-stretch band is split into two peaks, with the shape and intensities being almost identical for both salts. In a KSeCN and KSe^{13} solutiona in H_2O, two combination bands of the ion are visible – one between the CN–stretch and the SeCN bend and the other between the CN– and SeC–stretches (green line for KSeCN, blue line for KSe^{13}CN, both upscaled by ca. x50).

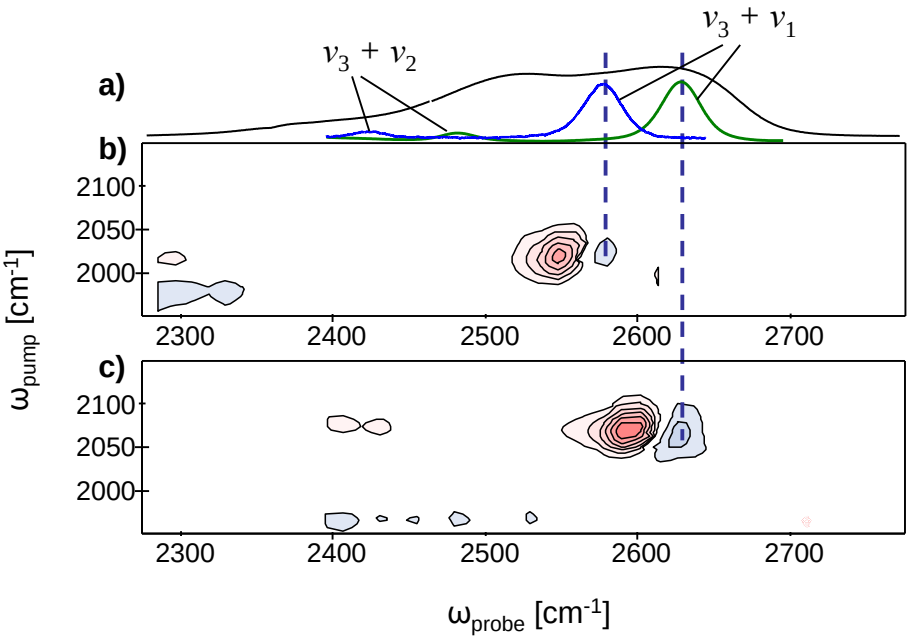

FIG. 7: KSeCN and KSe^{13}CN in D_2O. a) Linear spectra of the OD–stretch in KSeCN solutions in D_2O and the combination bands of KSeCN (green line) and KSe^{13}CN (blue line) b) 2D IR spectrum of KSe^{13}CN in D_2O at population time t_2=400 fs, c) 2D IR spectrum of KSeCN in D_2O at t_2=400 fs. Upon ^{13}C labeling, the 2D–IR cross–peaks shift not only in the pump frequency, ω_{pump}, but also in the probe frequency, ω_{probe}.